Periodic modulation of Coulomb-blockade oscillations in high magnetic fields

T. Heinzel, D. A. Wharam, and J. P. Kotthaus
Sektion Physik der Ludwig-Maximilians-Universität München, 80539 München, Germany

G. Böhm, W. Klein, G. Tränkle, and G. Weimann
Walter Schottky Institut, Technische Universität München, 85748 Garching, Germany
(Received 28 June 1994)

Coulomb-blockade oscillations in transport through a lateral quantum dot at small Landau-level filling factors are investigated. We observe both a periodic modulation of the peak conductance as well as a striking modulation of the peak separation. We show that below a Landau-level filling factor of 3 a single-particle description of these effects fails and the depopulation of the Landau levels with decreasing electron number can occur noncyclically. We interpret our measurements in terms of a recently developed phase diagram that characterizes the states of the quantum dot.

I. INTRODUCTION

Electronic transport studies through small conducting islands show several striking effects.[1] If the thermal energy $k_B T$ is small compared to the electrostatic energy required to add one additional electron to the island, conductance oscillations as a function of the electrochemical potential of the island are observed. These are usually called Coulomb-blockade (CB) oscillations,[1,2] whose period corresponds to the change of the number of electrons inside the island by 1. In our system, the conducting island is a quantum dot electrostatically defined in the two-dimensional electron gas (2DEG) of a GaAs-$Al_xGa_{1-x}As$ heterostructure. Additionally the dot is coupled to source and drain via two tunable tunnel barriers which permit the conductance to be measured. At source-drain bias voltages comparable to the discrete energy-level separation in the quantum dot, the amplitude of the CB oscillations depends upon the number of current-carrying states,[3,4] including excited states.[5] In the case of a small applied source-drain bias voltage, however, only one (possibly degenerate) quantum dot state carries current. The amplitude of the CB oscillation peak is then determined by the coupling of this particular state to the leads,[6,7] or by coherent resonant tunneling of the electrons through the quantum dot.[8]

In the presence of a magnetic field perpendicular to the plane of the 2DEG, the character of the CB oscillations is significantly modified. At Landau-level (LL) filling factors larger than 3, an amplitude modulation of the CB oscillations has been observed.[9] A description of the energy-level structure of the dot in terms of a single-particle picture leads to an excellent agreement with these experiments.[2,9] However, in the regime of Landau-level filling factor 2, it is well known that a single-particle model is unable to describe the experimental observations.[6,10] Magnetoconductance (MC) oscillations in this regime show a period that corresponds to the change of the magnetic flux within the area of the quantum dot by one flux quantum.[10] This indicates frequent crossings of the discrete energy levels not present in the single-particle spectrum. A quasi-self-consistent treatment of the quantum dot in this range of magnetic fields is able to explain the measurements. The minimization of a charge-density functional shows that the dot develops an additional electrostatic structure.[10–12] Within this model ["charge-density model" (CDM)], the formation of Landau levels leads to a modulation of the screening properties of the confined electrons,[13] and, as a consequence, the dot divides into compressible regions separated by incompressible rings. Recently, an analytical description of the quantum dot in terms of a phase diagram has been developed for the regime of LL filling factor below 2.[14] This description is based upon an analytic treatment of the charge-density distribution[13] inside the quantum dot; each phase is characterized by the number (n_1,n_2) of electrons at the Fermi energy in the different compressible regions.

Here we present measurements of CB oscillations over a wide range of magnetic fields (i.e., $2\ \mathrm{T} \le B \le 9\ \mathrm{T}$). At low magnetic fields ($B \le 3$ T), we observe an amplitude modulation which can become as large as 90% of the amplitude of the CB oscillation. At higher magnetic fields, we observe a periodic modulation of both the CB oscillation amplitude as well as their peak separations. We numerically extend the CDM to filling factors above 2 and apply these calculations to explain our experimental observations. We show that even at filling factors above 2, a single-particle description fails: the LL's are not always cyclically depleted when the electron number in the dot is reduced. In addition, we show that the period of MC oscillations is not necessarily given by the flux quantization condition.

II. EXPERIMENTAL DETAILS

For the fabrication of the quantum dot we use a $GaAs/Al_xGa_{1-x}As$ heterostructure with an electron density of $3.6\times10^{15}\ \mathrm{m}^{-2}$ and a mobility of $1.1\times10^{6}\ \mathrm{cm}^2/\mathrm{V\,s}$ at 4.2 K. The quantum dot is realized by the application of bias voltages to an appropriate gate structure defined on the surface of the heterostructure (Fig. 1). The

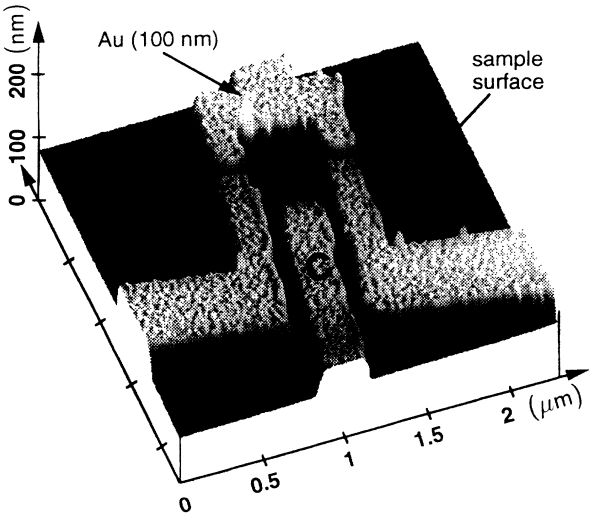

FIG. 1. Atomic force microscope picture of a typical gate structure (bright) on the surface of a GaAs-$Al_xGa_{1-x}As$ heterostructure (dark). The quantum dot is defined by application of negative gate voltages to the four electrodes. The arrow denotes the direction of current flow.

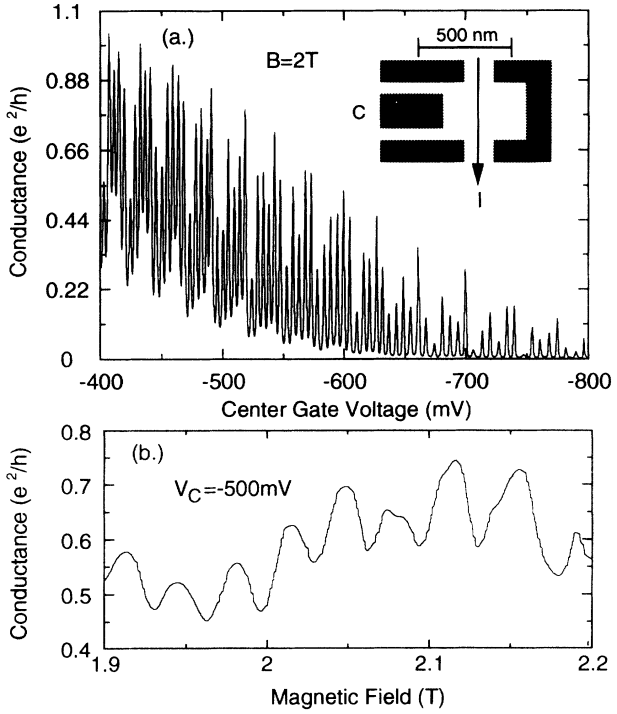

FIG. 2. (a) Conductance oscillations as a function of the center gate voltage V_C (inset) at $B=2$ T, corresponding to a filling factor of six inside the dot. The inset shows the schematic gate structure of our sample and the direction of the current I. The lithographic dot size is 450×480 nm^2. (b) Magnetoconductance oscillations at a fixed center gate voltage ($V_C=-500$ mV). The bath temperature for these measurements in (a) and (b) was $T=25$ mK.

electrodes form two quantum point contacts, whose transmission can be independently adjusted. For the experiments presented here, their conductance is kept fixed below $2e^2/h$. A sweep of the voltage applied to the center gate C leads to peaks in the conductance that are separated by e/C_C, where C_C is the partial capacitance between C and the dot. The total dot capacitance C_Σ is given by the sum of all the partial capacitances, including the capacitance between the quantum dot and the leads, C_L. For the structure considered here, we measure $C_\Sigma=200$ aF for typical gate voltages, where the capacitance C_L contributes 60 aF to C_Σ. We determine C_L from the difference between C_Σ as obtained from the temperature dependence of the linewidth of one CB oscillation conductance peak and the sum of all partial capacitances the dot forms with the gate electrodes.[4] The charging energy for a single electron is thus 0.4 meV. We apply an ac source-drain excitation voltage with an amplitude of 4.3 μV and measure the current in a two-terminal configuration. The current resolution is estimated to be 200 fA. The measurements are carried out in the mixing chamber of a dilution refrigerator with a base temperature of 25 mK.

III. RESULTS AND DISCUSSION

A. Low magnetic field—Darwin-Fock states

In Fig. 2(a), we show CB oscillations at $B=2$ T. A modulation of the peak conductance with an average period of six CB oscillations is observed. Similar behavior has been reported by Staring *et al.*[9] However, we see a much stronger modulation amplitude (90% compared to 10% in Ref. 9).[15] This amplitude modulation results from both the cyclic order in energy of the Darwin-Fock states[16] with respect to their LL index as well as the fact that only states belonging to the lowest LL couple to the leads. Due to both the increased length and height of the tunneling barrier, tunneling via higher Landau levels is strongly supressed and can be neglected.[9] For a given state at the Fermi level, the peak amplitude is thus modified by the occupation probability of the nearest state in energy of the lowest LL. The strength of the amplitude modulation is thus governed by the ratio between the typical energy-level separation and the thermal energy, $\delta E/k_BT$. For our sample, we estimate $\exp(-\delta E/k_BT)\approx0.1$. Assuming a typical electron temperature of $T\approx100$ mK, we expect a typical level separation of $\delta E\approx20\,\mu$ eV, in reasonable agreement with an estimation of δE using the Darwin-Fock model.

The MC at fixed gate voltages in this regime of the magnetic field is shown in Fig. 2(b). MC oscillations with a period of $\Delta B=37$ mT are measured. Within the model described above, one MC oscillation period corresponds to the addition of one electron to a state of LL 1. Hence, one flux quantum (h/e) must be added to the area of the dot. Assuming a circular dot shape, this allows us to estimate the dot radius to $r_{\rm dot}=\sqrt{h/\pi e\Delta B}\approx190$ nm, in good agreement with the lithographic dimensions combined with electrostatic depletion lengths.

B. High magnetic field—introduction to the phase diagram

In Sec. III C, we discuss the properties of the CB oscillations for filling factors inside the quantum dot $\nu_{dot} \leq 2$, i.e., $B \geq 6$ T. At $B=6$ T, we observe an amplitude modulation with a period of two conductance peaks. The peak separations are modulated with the same period [Fig. 3(a)]. This behavior[10] can be understood in terms of the CDM.[14] The compressible regions I and II are separated by an incompressible ring, located at the region of unity filling factor [Fig. 3(b)]. Hence, an additional intradot capacitance arises which is responsible for the observed modulation of the peak separation. Within the CDM, the state of the dot in the regime $\nu_{dot} \leq 2$ has been characterized in terms of a phase diagram. Each phase is characterized by the number (n_1,n_2) of electrons in the outermost compressible region I and in the innermost compressible region II, respectively. An obvious requirement for the existence of well-defined compressible regions is that the magnetic length, $l_B=\sqrt{\hbar/eB}$, be smaller than the separation between these regions. In Ref. 14, the intradot capacitance C_{12} is assumed to be constant, and the capacitance C_L [see Fig. 3(b)] between the dot and the leads is neglected. The value of C_L determined from the temperature dependence of the CB oscillation line shape[4] is for the sample considered 60 aF. This is approximately 30% of C_Σ and certainly not negligible. To include the influence of a significant C_L as well as the magnetic-field dependence of the intradot capacitance C_{12}, we have minimized numerically the total electrostatic energy of the quantum dot in the plane defined by C_{1C} and V_C. We have modeled the dependence of C_{12} on C_{1C} using the expressions developed in Ref. 13 [Fig. 3(c)]. Since the area of region I is a monotonically increasing function of magnetic field, we note that C_{1C} can be identified, within a certain range of validity, with a magnetic field. The symmetry of the phase diagram around $C_{1C}=C_{2C}$ (Ref. 14) is removed by a non-negligible value of C_L. Furthermore, as a consequence of the decreasing value of C_{12} with increasing C_{1C}, the amplitude of the zigzag line that separates phases belonging to a different total number of electrons inside the dot increases. The modulation of the peak separation reflects the different lengths of the traversed phases under a variation of the applied gate voltage at a fixed value of the magnetic field. The amplitude of the CB oscillations is determined by the coupling between region I and the leads. Note that only region I carries current, since the overlap of the wave functions between regions I and II is negligible. As in the

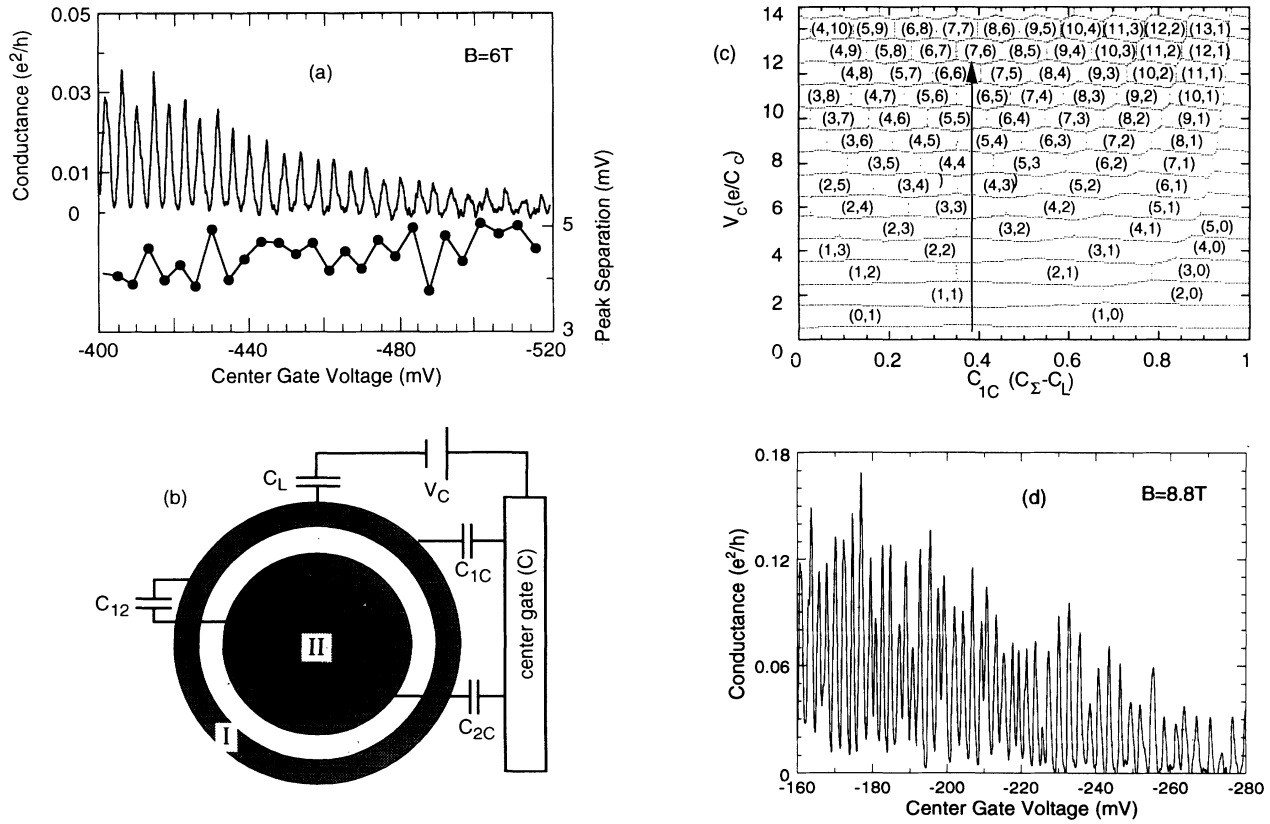

FIG. 3. (a) CB oscillations at filling factor $\nu_d \leq 2$ ($B=6$ T) and the corresponding peak separations at $T=25$ mK. (b) The structure of the electron gas inside the dot as obtained from the charge-density model. An intradot capacitance C_{12} between the compressible regions I and II is formed, separated by an incompressible ring. Each compressible zone has a partial capacitance with respect to the gates and contains an integer number of electrons, n_i, $i=1$ and 2. (c) Calculated phase diagram of the quantum dot for $\nu_d \leq 2$. The capacitance between the outermost region I and the leads was assumed to be $0.3C_\Sigma$. The arrow denotes a center gate voltage sweep at fixed magnetic field. (d) CB oscillations at $B=8.8$ T and $T=25$ mK.

low-field case discussed above in Sec. III A, the electronic transport occurs via activated states of LL 1.

The maximum amplitude $\delta(\Delta V_C)$ of the zigzag-shaped phase boundaries separating regions that contain a different total number n_1+n_2 is given by[14]

$$\delta(\Delta V_C)_{\max} \leq \frac{e}{4C_{12}+C_\Sigma} . \quad (1)$$

To compare Eq. (1) quantitatively with the measurements, we determine the conversion ratio $\alpha=\Delta E/e\Delta V_C=C_C/C_\Sigma$, with $C_C=e/\Delta V_C$, where ΔV_C is the mean separation of the conductance peaks. We see a strong dependence of ΔV_C on V_C. This effect has its origin in the decreasing value of C_C with decreasing V_C, as a consequence of the increasing depletion length between the dot and C. In the regime between -900 mV $< V_g < -300$ mV we find, independent of the applied magnetic field, a linear dependence of ΔV_C on V_C, which we fit by $\Delta V_C=1.2\times10^{-3}$ V $-7.3\times10^{-3}\times V_C$. From Fig. 3(a), we determine at $V_C=-480$ mV $\delta(\Delta V_C)_{\max}=0.6$ mV, leading to an estimation for $C_{12}\leq 380$ aF. This value may be compared directly with the intradot capacitance C_{12} as obtained from electrostatic considerations.[14] We approximate C_{12} by

$$C_{12}=4\varepsilon\varepsilon_0 r_1 \ln\left[\frac{4d}{w_1}\right] , \quad (2)$$

where d is the typical width of the compressible regions ($d\approx 100$ nm), and r_1 is the radius of the middle of the incompressible ring. Using the expressions derived in Ref. 14, we calculate $r_1=130$ nm at $B=6$ T. Equation (2) can be used to estimate the width of the incompressible ring to $w_1\geq 10$ nm. This width depends upon the separation of the lowest two LL's, which is given by the effective g factor g_{eff}. Hence we can estimate $g_{\text{eff}}\geq 3$. Furthermore, we see that the intradot capacitance is comparable to the other capacitances in our system.

MC oscillations in this regime show the same period as those at much lower magnetic fields [Fig. 2(b)] and represent the transfer of electrons from region II into region I.[7,10–12,17] Since the intradot charging energy $e^2/2C_{12}$ is much smaller than the Zeemann splitting, this electron transfer is governed by the flux quantization condition discussed above.

Another interesting feature of this phase diagram which is reproduced in our measurements is the behavior at extremely high magnetic fields. As expected from Fig. 3(c), the periodicity of the peak separation modulation is absent at magnetic fields much higher than 6 T [Fig. 3(d)]. Since the number of electrons contained in regions I and II is very different, the two compressible regions are no longer cyclically depleted under the variation of the center gate bias.

C. Extension of the phase diagram to intermediate magnetic fields

At intermediate filling factors, i.e., $2<\nu_d\leq 3$, we observe both a cyclic depopulation of the LL's [Fig. 4(a)] as well as modulations that indicate a noncyclic depopulation [Fig. 4(c)]. At $B=4$ T, the period of three CB oscillations indicates a filling factor inside the dot of $\nu_d=3$. In this regime, we clearly resolve the spin splitting and observe additionally a striking modulation of the CB oscillation peak separations. A single-particle description is not able to explain these measurements. Modeling the dot by Darwin-Fock states and under the assumption of a reasonable enhanced g factor, it is impossible to occupy states in the third LL while leaving the fourth LL unoccupied. These measurements are therefore a clear indication of the necessity to include the Coulomb interaction to explain these data. Note also that the sequence of depopulation sometimes changes [Fig. 4(a)]. Hence the LL's are no longer strictly cyclically depopulated. The quasicyclic depopulation of the Landau levels is completely lost in a magnetic field of $B=5$ T [Fig. 4(c)]. In terms of the charge-density distribution model, such a noncyclic depopulation is readily understood. For filling factors between 2 and 3 it is to be expected that the dot decomposes into three compressible regions, each with an integer number of electrons at the Fermi energy. If the three compressible rings are equal in area, their electron occupation numbers n_1, n_2, and n_3 will be approximately the same. If, however, one region is large or small compared to the remaining ones, a cyclic depopulation is no longer energetically favorable. At $B=5$ T, the area of the innermost region (III) is close to zero. Hence we expect n_3 to be small compared to both n_1 and n_2, and consequently a noncyclic depopulation of the compressible regions occurs.

To justify this interpretation, we have extended the phase diagram [Fig. 3(c)] (Ref. 14) to the case of three compressible regions. At each value of C_{1C} and V_C, we minimize the total electrostatic energy of the dot numerically. This calculation gives the distribution of the electrons among the compressible regions, where each phase is now characterized by three numbers (n_1, n_2, and n_3). As above, we include the capacitance between region I and the leads. Figures 4(b) and 4(d) show two sections of the calculated phase diagram. Not only do we find regions of cyclic depopulation, but also, at small values of C_{3C}, noncyclic depopulation of the three compressible regions. In detail, we choose C_{2C} and C_{3C} to decrease linearly with increasing C_{1C}. We include the behavior of the intradot capacitances using Eq. (2). Despite the large uncertainties of these phase boundaries due to both the crude estimations of the capacitances as well as the limited range of validity of Eq. (2), these calculations are able to explain the experimental observations qualitatively.

D. Magnetoconductance oscillations and flux quantization

The period of MC oscillations is usually explained with the flux quantization. If the magnetic field is increased, the charge flows toward the center of the dot, and, hence, the electrochemical potential in the outermost compressible region, μ_1, decreases, while it increases in the inner regions. Once an additional flux quantum has been added to the area of the dot, an electron can be transferred from an inner region to the outermost region I, thereby reduc-

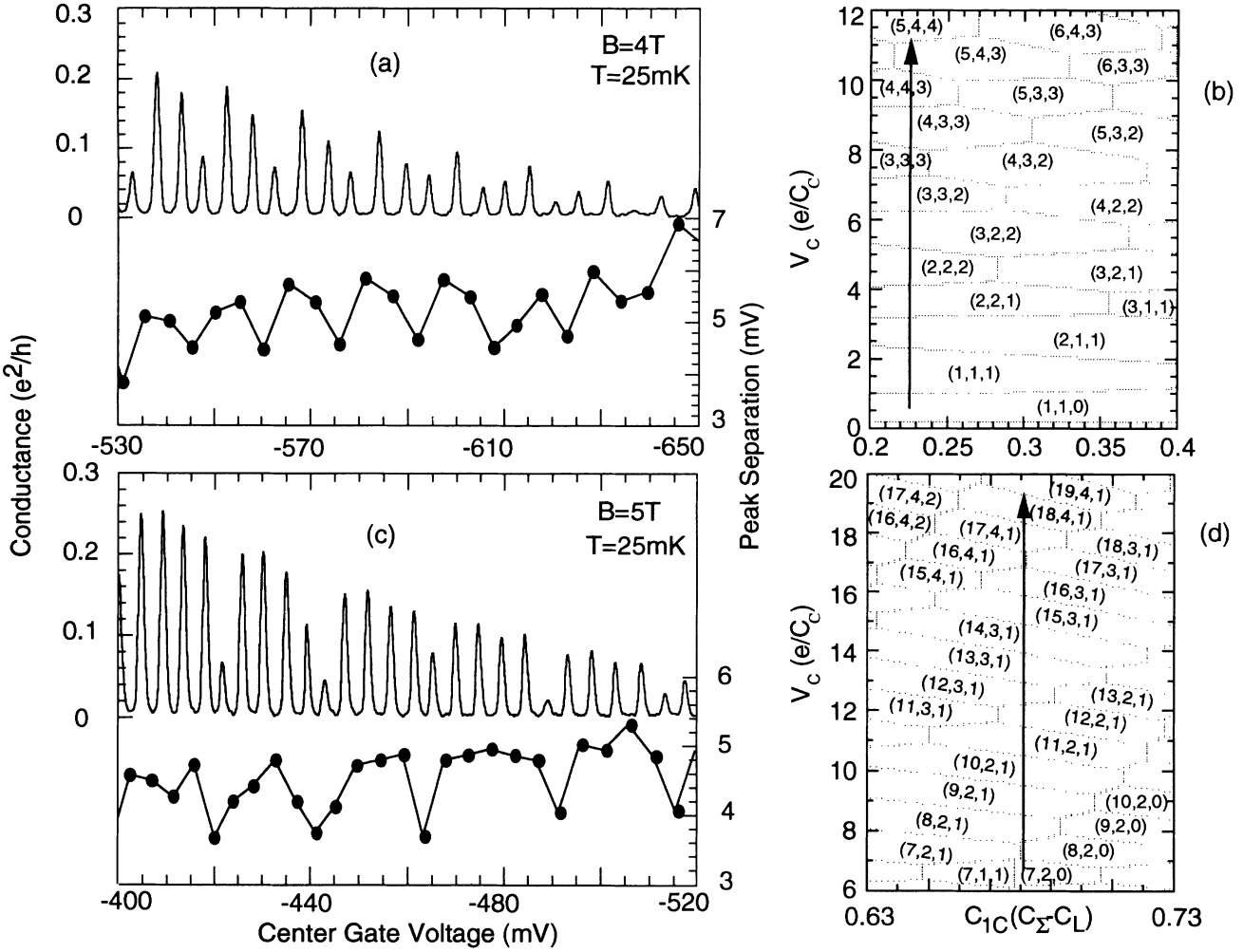

FIG. 4. (a) CB oscillations at $B=4$ T and their peak separations. (b) The corresponding section of a generalized phase diagram as numerically calculated. (c) At $B=5$ T, a noncyclic depopulation of the Landau levels is found. (d) This behavior at $B=5$ T can also be modeled by the phase diagram description, and corresponds to a much higher value of C_{1C}.

ing the total electrostatic energy of the dot. Since the difference between the electrochemical potential in region I and in the leads can be taken as a measure of the coupling of I to the leads, this electron transfer is reflected in the conductance of the quantum dot. Moreover, one expects the number of electrons in the dot to decrease slowly as a function of increasing magnetic field.[17] Hence one expects to observe broad resonances with a short-period oscillation superposed[17] [Fig. 5(a)]. To bring the dot back into a conducting state after crossing one broad resonance, it is necessary to change the number of electrons inside the dot. One broad resonance thus corresponds to the magnetic-field interval necessary to change the occupation number of the dot by one electron.[17]

If one compressible region becomes very small, the associated charging energy necessary to transfer one electron can exceed the energy separation of the LL's. In this case, the period of the MS oscillations is no longer determined solely by the flux quantization condition, but also by the intradot charging energies.

As expected, we observe broad resonances with a separation of approximately 0.5 T superposed with short-period oscillations. For the resonance at 3.15 T, the short period has a mean value of $\Delta B=35$ mT, in good agreement with our low-field data [Fig. 2(b)]. Within this short period two distinct peaks are clearly visible. At $B=3.15$ T the filling factor of the dot lies between $3\leq\nu_d\leq 4$. As the magnetic field is increased, electrons contained in the uppermost two LL's are cyclically transferred to LL's 1 and 2. Within one modulation period ($\Delta B=35$ mT), one flux quantum is added to the area of the quantum dot. This allows the addition of one electron to both LL's 1 and 2. If an electron is added to LL 1, the change in the conductance is large. If, however, the electron is added to LL 2, μ_1 is only slightly changed due to the capacitive coupling between regions I and II, and hence the corresponding conductance peak is small.

The short-period oscillation in the resonance around $B=3.65$ T, however, cannot be attributed to the area of the quantum dot. One possible explanation is that, in this regime, the electrostatic energy needed for a rearrangement of the electrons becomes comparable to the magnetic energies in the dot. At $B=3.65$ T, the fourth

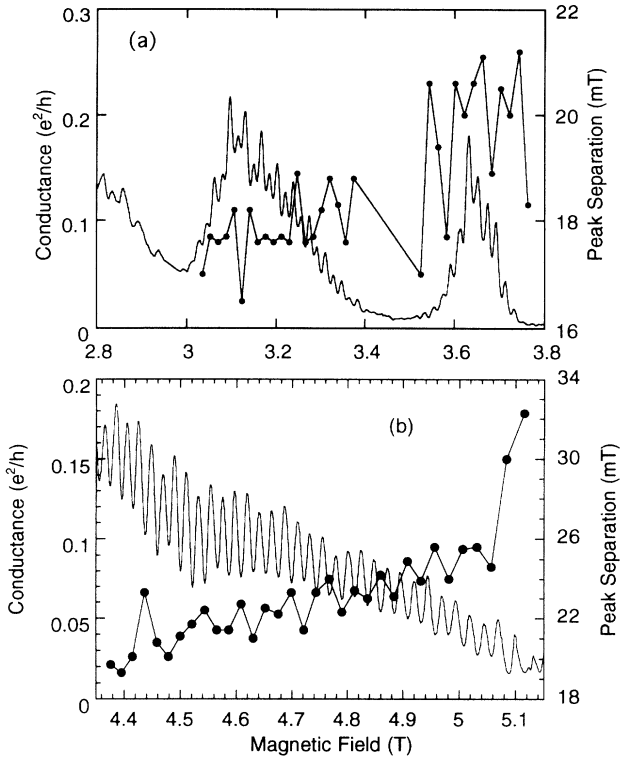

FIG. 5. Magnetoconductance oscillations and the corresponding periods at fixed center gate voltages [$V_C = -600$ mV in (a) and $V_C = -505$ mV in (b)] at a bath temperature of $T = 25$ mK.

LL is nearly completely depleted. We thus expect a very small intradot capacitance between the compressible regions III and IV.

Around $B = 5$ T, a noncyclic depopulation of the LL's is found in center gate voltage sweeps [Fig. 4(c)]. This indicates that the innermost compressible region III has a very small area. We can thus expect that the cyclotron energy is comparable to e^2/C_{23}. In this regime, we find a MC oscillation whose period increases with increasing magnetic field. The increase in period thus reflects the decrease of C_{23} with increasing magnetic field. In addition, we observe a slight modulation in the MC oscillation peak separation with a period of two oscillation peaks. We take this as an indication that the electrons in region III are cyclically transferred into regions I and II. The last observable oscillations in this measurement at $B \approx 5.1$ T show a significantly increased peak separation. An explanation for this behavior might be that we observe the complete depletion of region III. If the mean separation of the electron in region III exceeds the magnetic length, the charge density is no longer homogeneous. Indeed, the formation of a "Wigner molecule" has recently been predicted.[18] An unambiguous verification of this effect would require a pronounced hysteresis of the CB oscillations with respect to the gate voltage sweep direction.[18] Such behavior has not been observed in our measurements.

IV. CONCLUSIONS

In summary, we have investigated Coulomb-blockade oscillations in a semiconductor quantum dot at high magnetic fields, and have found strong modulations both in the amplitude as well as in the separation of the conductance peaks. At filling factors between 2 and 3, our measurements show that a description of the quantum dot in terms of a single-particle model is unable to explain the observed modulation of the peak conductances. A generalization of the recently developed description of the dot in terms of a phase diagram to the regime of filling factor 3 reproduces all of the experimental observations. The depletion of the LL's does not always occur cyclically, and the period of the magnetoconductance oscillations is not always determined by the flux quantization condition, but presumably by the energies necessary to change the distribution of the electrons inside the dot.

ACKNOWLEDGMENTS

It is a pleasure to thank V. Dolgopolov for many fruitful discussions, and S. Manus for his expert help in developing the measurement electronics. This work was financially supported by the Deutsche Forschungsgemeinschaft.

[1]For a review, see the special issue on single charge tunneling, in Z. Phys. B **85** (3) (1991).
[2]C. W. J. Beenakker, Phys. Rev. B **44**, 1646 (1991).
[3]A. T. Johnson, L. P. Kouwenhoven, W. de Jong, N. C. van der Vaart, C. J. P. M. Harmans, and C. T. Foxon, Phys. Rev. Lett. **69**, 1592 (1992).
[4]E. B. Foxman, P. L. McEuen, U. Meirav, Ned S. Wingreen, Yigal Meir, Paul A. Belk, N. R. Belk, M. A. Kastner, and S. J. Wind, Phys. Rev. B **47**, 10020 (1993).
[5]J. Weis, R. J. Haug, K. v. Klitzing, and K. Ploog, Phys. Rev. Lett. **71**, 4019 (1993).
[6]P. L. McEuen, E. B. Foxman, U. Meirav, M. A. Kastner, N. S. Wingreen, and S. J. Wind, Phys. Rev. Lett. **66**, 1926 (1991).
[7]J. M. Kinaret and N. S. Wingreen, Phys. Rev. B **48**, 11113 (1993).
[8]T. Heinzel, S. Manus, D. A. Wharam, J. P. Kotthaus, G. Böhm, W. Klein, G. Tränkle, and G. Weimann, Europhys. Lett. **26**, 689 (1994).
[9]A. A. M. Staring, B. W. Alphenaar, H. van Houten, L. W. Molenkamp, O. J. A. Buyk, M. A. A. Mabesoone, and C. T. Foxon, Phys. Rev. B **46**, 12869 (1992).
[10]P. L. McEuen, E. B. Foxman, J. Kinaret, U. Meirav, M. A. Kastner, N. S. Wingreen, and S. J. Wind, Phys. Rev. B **45**, 11419 (1992).
[11]I. K. Marmorkos and C. W. J. Beenakker, Phys. Rev. B **46**, 15562 (1992).

[12]Yigal Meir, Ned S. Wingreen, and Patrick A. Lee, Phys. Rev. Lett. **66**, 3048 (1991).

[13]D. B. Chklovskii, B. I. Shklovskii, and L. I. Glazman, Phys. Rev. B **46**, 4026 (1992).

[14]A. K. Evans, L. I. Glazman, and B. I. Shklovskii, Phys. Rev. B **48**, 11 120 (1993).

[15]T. Heinzel, D. A. Wharam, S. Manus, J. P. Kotthaus, G. Böhm, W. Klein, G. Tränkle, and G. Weimann, in *Proceedings of the IVth Rencontres de Moriond, Condensed Matter Physics Meeting, April 1994,* edited by D. C. Glattli and M. Sanquer (Editions Frontières, Paris, 1994).

[16]C. G. Darwin, Proc. Cambridge Philos. Soc. **27**, 86 (1931); V. Fock, Z. Phys. **47**, 446 (1928).

[17]N. C. van der Vaart, M. P. de Ruyter van Stevenick, C. J. P. M. Harmans, and C. T. Foxon, Physica B **194-196**, 1251 (1994).

[18]Yu. Nazarov and A. Khaetskii, Phys. Rev. B **49**, 5077 (1994).

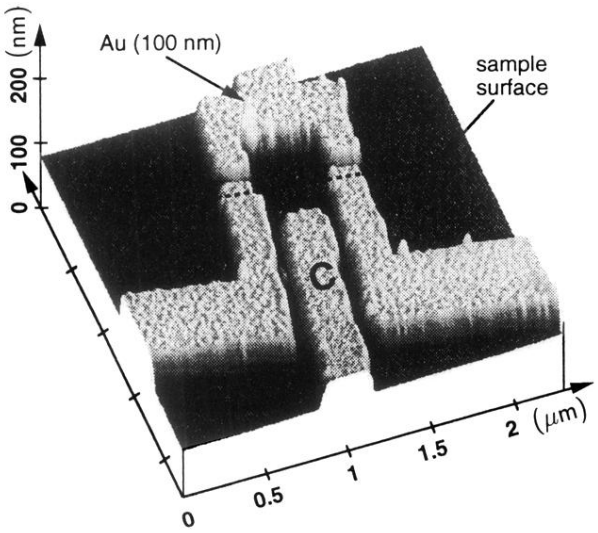

FIG. 1. Atomic force microscope picture of a typical gate structure (bright) on the surface of a GaAs-$Al_xGa_{1-x}As$ heterostructure (dark). The quantum dot is defined by application of negative gate voltages to the four electrodes. The arrow denotes the direction of current flow.

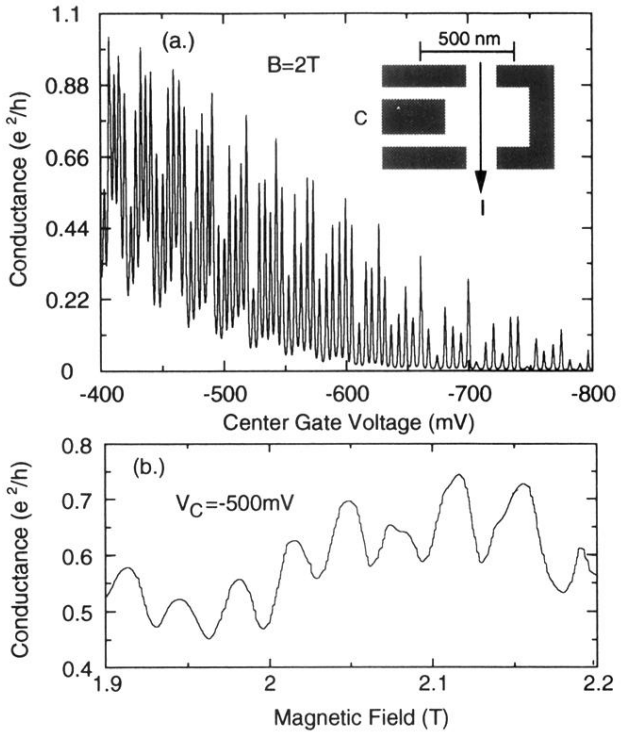

FIG. 2. (a) Conductance oscillations as a function of the center gate voltage V_C (inset) at $B=2$ T, corresponding to a filling factor of six inside the dot. The inset shows the schematic gate structure of our sample and the direction of the current I. The lithographic dot size is 450×480 nm^2. (b) Magnetoconductance oscillations at a fixed center gate voltage ($V_C=-500$ mV). The bath temperature for these measurements in (a) and (b) was $T=25$ mK.

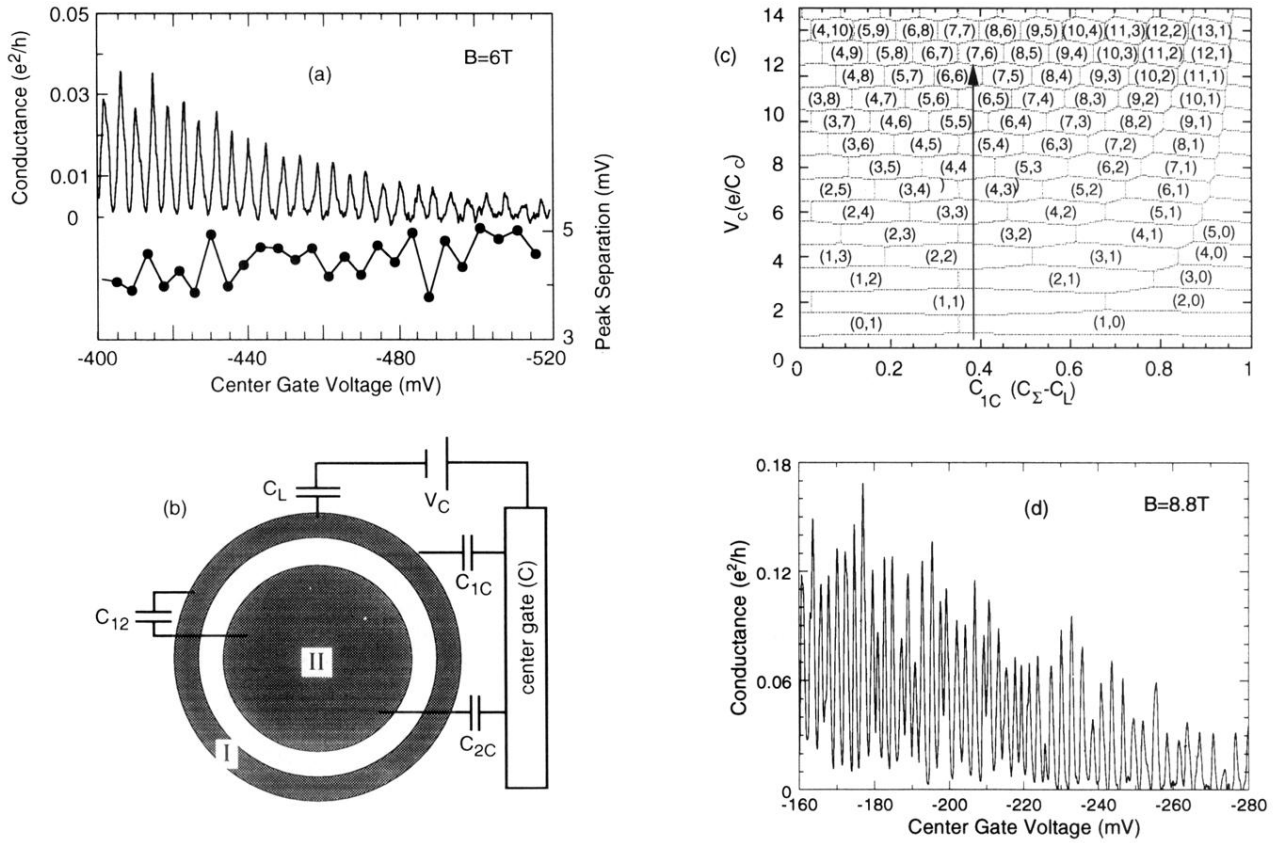

FIG. 3. (a) CB oscillations at filling factor $\nu_d \leq 2$ ($B=6$ T) and the corresponding peak separations at $T=25$ mK. (b) The structure of the electron gas inside the dot as obtained from the charge-density model. An intradot capacitance C_{12} between the compressible regions I and II is formed, separated by an incompressible ring. Each compressible zone has a partial capacitance with respect to the gates and contains an integer number of electrons, n_i, $i=1$ and 2. (c) Calculated phase diagram of the quantum dot for $\nu_d \leq 2$. The capacitance between the outermost region I and the leads was assumed to be $0.3C_\Sigma$. The arrow denotes a center gate voltage sweep at fixed magnetic field. (d) CB oscillations at $B=8.8$ T and $T=25$ mK.